Far-field acoustic prediction using the boundary element method and robotized measurements

Caroline PASCAL

U2IS & UME – ENSTA Paris

December 7&8, 2023

Did you say far-field acoutsic prediction ?

Objective

Predict the far-field acoustic quantities radiated by an unknwon sound source, based on a set of near-field measurements.

Idea

Combine robotized measurements and the boundary elements method (BEM).

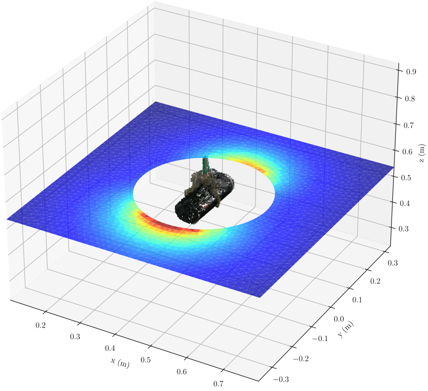

Figure 1: Example of far-field acoustic pressure prediction on a JBL Flip 2 at 50 *Hz*

Table of Contents

Table of Contents

Robotized acoustic measurements

→ **An increasing need of high numbered 3D measurements.**

→ **A shy use of robots in acousitcs.**

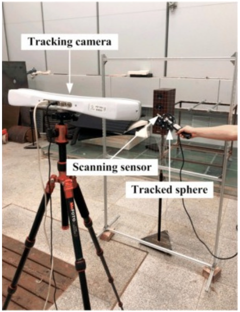

Figure 2: 3D tracked [1] and array based [2] acoustic measurements

Figure 3: Planar robotized acoustic measurements [3]

⟹ **Objective**: investigate the use of a robotic arm to perform numerous and autonomous 3D acoustic measurements.

Robotized acoustic measurements setup

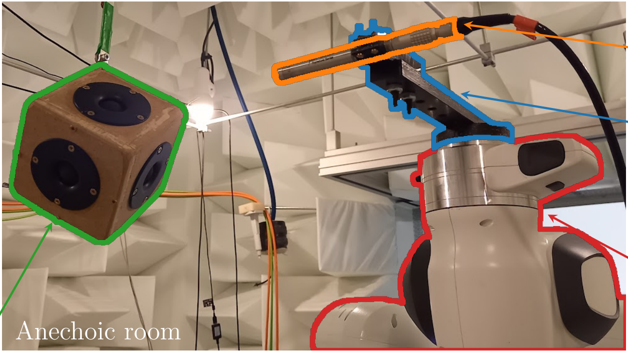

Robotized acoustic measurements: Pros and Cons

→ Pros

- High positionning flexibility, with 6 degrees of freedom (position and rotation).
- Fully-autonomous measurements, with no required human intervention.

→ Cons

- The studied sound source must be repeatable and stable over time. ✓
- The robot positionning accuracy (± 2 mm) must be taken into account [4]. ✓
- The robot acoustic footprint must also be assessed.

Robot acoustic footprint: the bull in the china shop ?

→ **Idea**: compare the acoustic measurements *with* and *without* the robot in several control configurations.

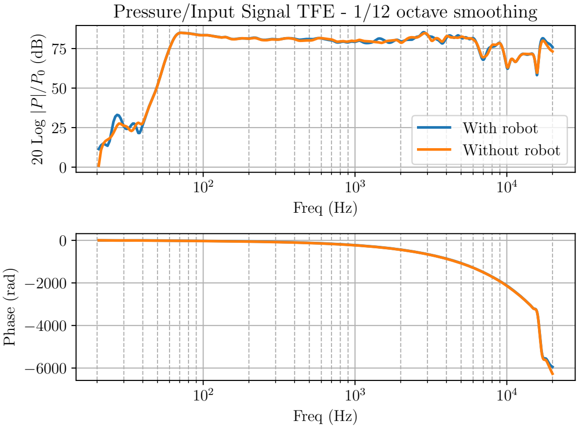

Figure 4: Transfer functions - 10 *s logsweep on a JBL Flip 2 sampled at* 96 *kHz*, *Welch's method and* 12^{th} *octave smoothing*

Robot acoustic footprint: the bull in the china shop ?

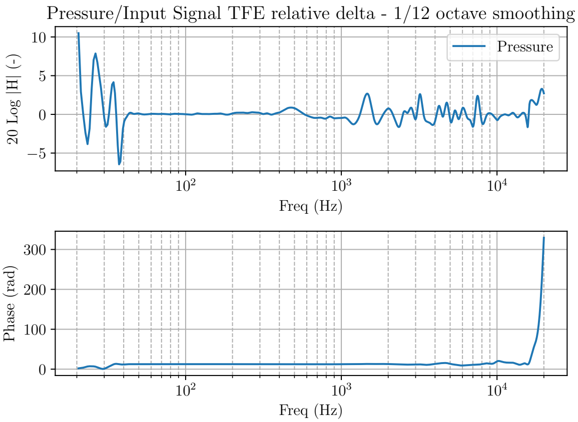

Figure 5: Transfer functions relative delta

$\Longrightarrow$ The 40 *Hz* - 1 *kHz* frequency range is considered valid for acoustic measurements ($\Delta < 3\ dB$).

Table of Contents

The Boundary Elements Method (BEM)

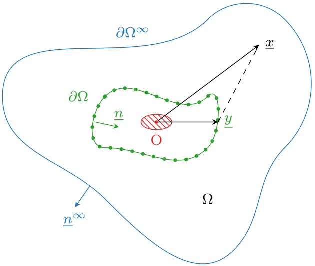

Helmholtz free-field equation with Sommerfeld radiation condition

$$\begin{cases} \Delta p(\underline{x}) + k^2 p(\underline{x}) = 0 & \text{in} \quad \Omega \\ p(\underline{x}) = p_0(\underline{x}) & \text{on} \quad \partial\Omega \\ \lim\limits_{\partial\Omega^\infty \to \infty} \left(\frac{\partial}{\partial |x|} - ik \right) p(\underline{x}) = 0 & \end{cases} \tag{1}$$

→ *Exterior Dirichlet problem for Helmholtz equation*

The Boundary Elements Method (BEM) [5]

Single layer potential associated to the Helmholtz equation

$$\forall\ \underline{x} \in \Omega \setminus \partial\Omega,\ S(\phi)(\underline{x}) = \int_{\partial\Omega} G(\underline{x}, \underline{y})\phi(\underline{y})d\sigma(\underline{y})$$

Where $G(\underline{x}, \underline{y}) = \frac{\exp ik|\underline{x}-\underline{y}|}{4\pi|\underline{x}-\underline{y}|}$ is the free-field Green function, and $\phi \in H^{-1/2}(\partial\Omega)$ defines a boundary density.

$\rightarrow S(\phi)$ is a solution of (1), provided that ϕ is such that the boundary conditions are satisfied.

Boundary conditions integral formulation

$$\exists\ \phi : \partial\Omega \rightarrow \mathbb{C},\ \forall\ x \in \partial\Omega,\ \gamma_0 p(\underline{x}) = p_0(\underline{x}) = \int_{\partial\Omega} G(\underline{x}, \underline{y})\phi(\underline{y})d\sigma(\underline{y}) \quad (2)$$

Where γ_0 describes the Dirichlet trace operator.

⚠ Some values of k lead to spurious resonances while solving (2) !

The Boundary Elements Method (BEM)

Double layer potential associated to the Helmholtz equation

$$\forall\ \underline{x} \in \Omega \setminus \partial\Omega,\ \ D(\phi)(\underline{x}) = \int_{\partial\Omega} \frac{\partial G(\underline{x}, \underline{y})}{\partial \underline{n}(\underline{y})} \phi(\underline{y}) d\sigma(\underline{y})$$

Combined layer potential associated to the Helmholtz equation [6]

$$\forall\ \underline{x} \in \Omega \setminus \partial\Omega,\ \ C(\phi)(\underline{x}) = D(\phi)(\underline{x}) - ikS(\phi)(\underline{x})$$

→ $C(\phi)$ is a resonance free solution of (1), provided that ϕ is such that the boundary conditions are satisfied.

Boundary conditions integral formulation

$$\exists\ \phi : \partial\Omega \to \mathbb{C},\ \forall\ x \in \partial\Omega,$$

$$p_0(\underline{x}) = \left(\frac{\phi(\underline{x})}{2} + \int_{\partial\Omega} \frac{\partial G(\underline{x}, \underline{y})}{\partial \underline{n}(\underline{y})} \phi(\underline{y}) d\sigma(\underline{y}) \right) - ik \int_{\partial\Omega} G(\underline{x}, \underline{y}) \phi(\underline{y}) d\sigma(\underline{y})$$

Numerical assessment setup

- `FreeFem++` [7] implementation of the combined boundary integral equation resolution (`BemTool` & `Htool` libraries).

  → Linear surface elements and P_0 Lagrange elements.

- **Near-field measurements** simulated on a **spherical mesh** of diameter 50 *cm* and variable resolution.

  → A geodesic polyhedron primitive is used to ensure a uniform distribution of the vertices.

- **Far-field prediction** computed on a **circular mesh** of diameter 1 *m* containing 100 vertices.

Numerical assessment: the acoustic monopole

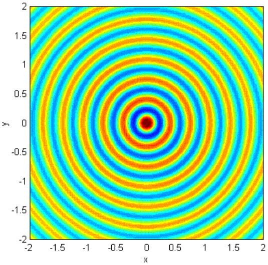

Acoustic monopole

$$p_M(\underline{x}) = \frac{\exp ik|\underline{x} - \underline{x}_0|}{4\pi|\underline{x} - \underline{x}_0|}$$

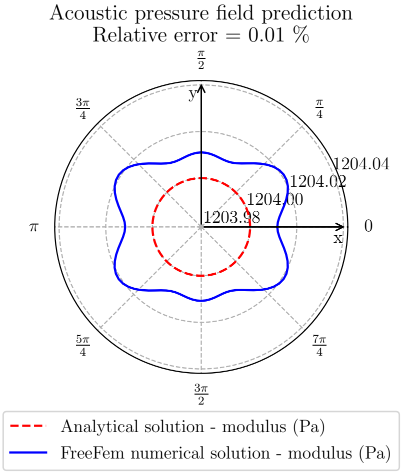

Figure 6: Prediction results obtained at 1 *kHz*, with a 5 *mm* resolution

Numerical assessment: convergence

→ L_2 prediction error theoretical convergence behaviour for linear surface elements and P_0 Lagrange elements: $O(h^2)$ [8][9]

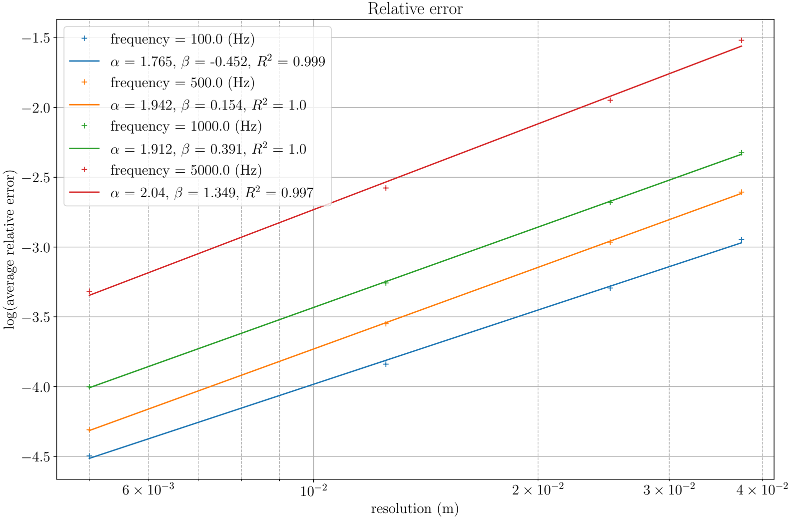

Numerical assessment: the acoustic dipole

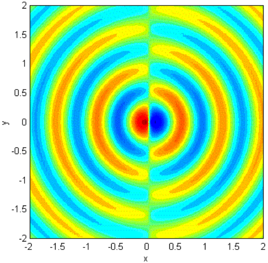

Acoustic dipole

$$p_D(\underline{x}) = p_M(\underline{x} + \underline{\delta}) - p_M(\underline{x} - \underline{\delta})$$

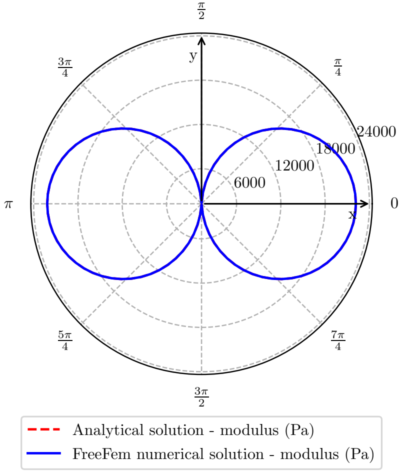

Figure 7: Prediction results obtained at 1 kHz, with a 5 mm resolution

Numerical assessment: convergence

→ L_2 prediction error theoretical convergence behaviour for linear surface elements and P_0 Lagrange elements: $O(h^2)$ [8][9]

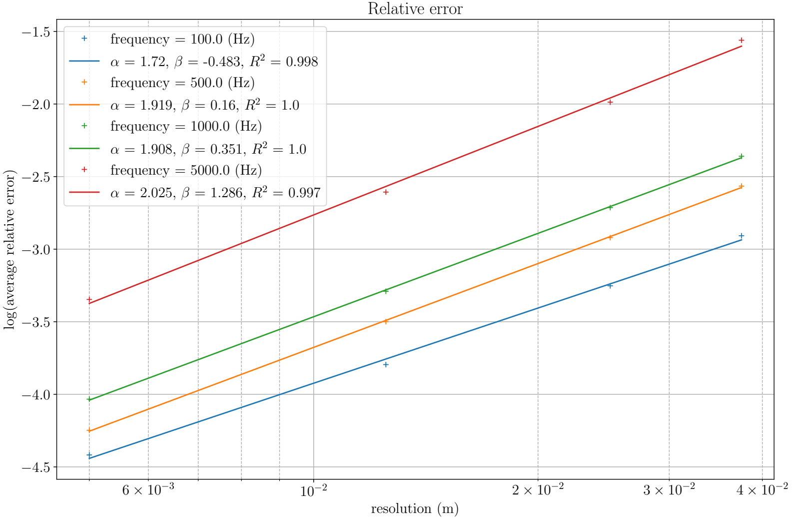

Numerical assessment: and when the robot steps in ?

→ Study of the impact of the robot positionning inaccuracies, by adding a gaussian noise ($\sigma = 1,25\ mm$) on the mesh vertices position.

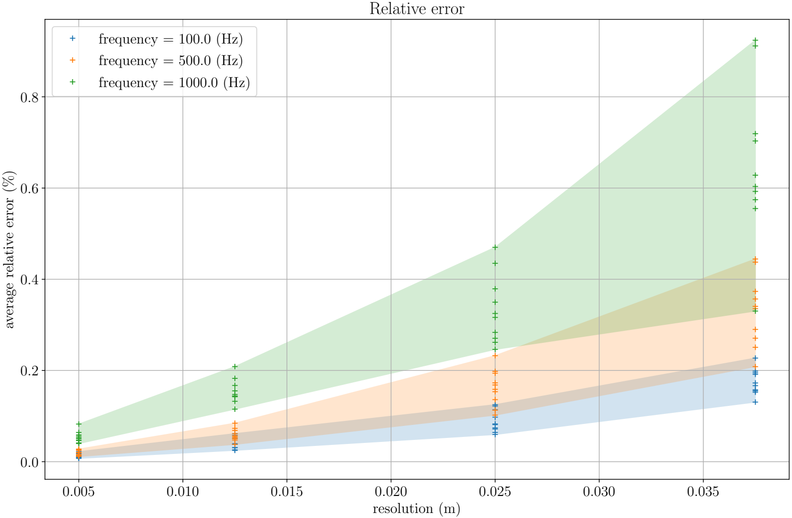

Table of Contents

Robotized acoustic measurements

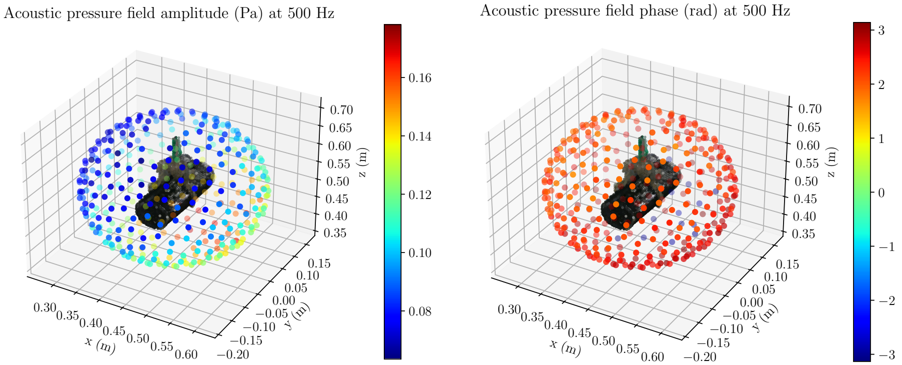

Figure 8: Sound pressure levels and phase measured at 500 *Hz* for each measured position, using a JBL Flip 2

372 measurements, spherical mesh of diameter 35 *cm and resolution* 5 *cm (total duration* ±2 *h)*

BEM based Far-field acoustic prediction

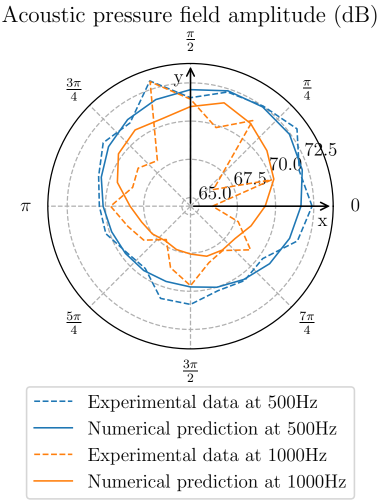

Figure 9: Predicted and measured sound pressure levels at 500 *Hz* and 1000 *Hz*
20 measurements, circular trajectory of diameter 50 *cm at* $z = 0$ *cm*

BEM based Far-field acoustic prediction

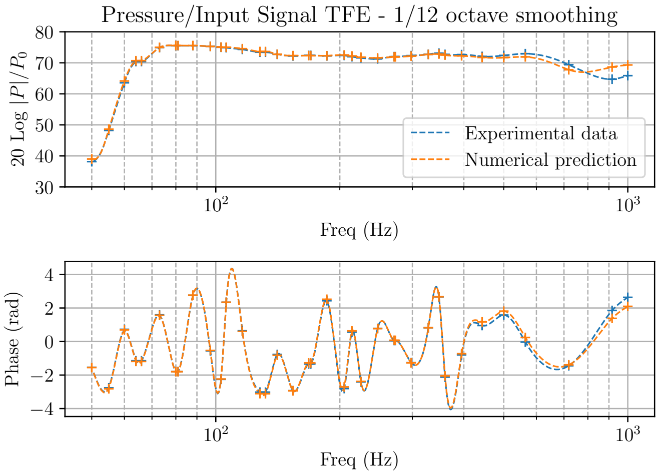

Figure 10: Predicted and measured data over the measurements frequential validity range

Measurement at $x = 25$ cm and $y = 0$ cm

BEM based Far-field acoustic prediction

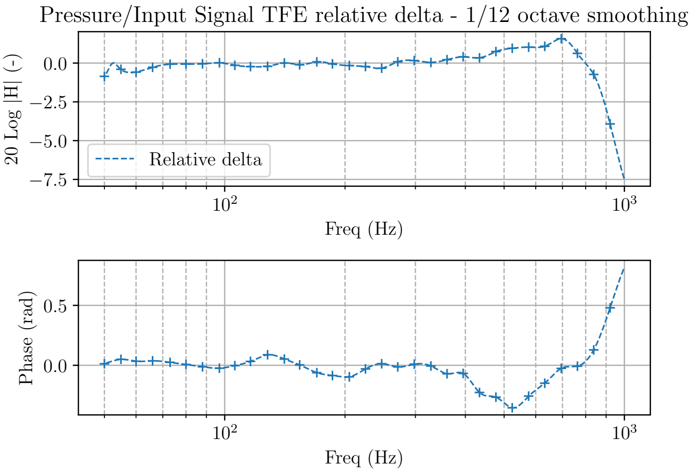

Figure 11: Predicted and measured data relative delta over the measurements frequential validity range
Measurement at $x = 25$ cm and $y = 0$ cm

Table of Contents

Projected work and perspectives

- **Reduce the prediction errors at high frequencies**

  → Reduce the robot acoustic footprint and the distance between measurements to increase accuracy.

  → **Use higher order surface elements**, and shape functions.

- **Tackle the near-field acoustic holography problem**

  → Inverse problem: how about the acoustic field close to the source ?

  → Requires **regularization while solving the boundary integral equation** (PETSc - TAO !).

- **Furhter investigate sound field derivatives**

  $\implies$ In acoustic, the pressure gradient is proportionnal to the particle velocity.

  → How about the implementation of the **"derivatives" of the single and double layers potentials** ?

Conclusion

Thank you for your time and attention !

robot_arm_acoustic

References I

Zhong-Wei Luo, Daniel Fernandez Comesana, Chang-Jun Zheng, and Chuan-Xing Bi.
Near-field acoustic holography with three-dimensional scanning measurements.
Journal of Sound and Vibration, 2019.

Hanwen Bi, Fei Ma, Thushara D. Abhayapala, and Prasanga N. Samarasinghe.
Spherical array based drone noise measurements and modelling for drone noise reduction via propeller phase control.
In *2021 IEEE Workshop on Applications of Signal Processing to Audio and Acoustics (WASPAA)*, 2021.

References II

Mélanie Nolan, Samuel Verburg, Jonas Brunskog, and Efren Fernandez-Grande.
Experimental characterization of the sound field in a reverberation room.
The Journal of the Acoustical Society of America, 2019.

Caroline Pascal, Alexandre Chapoutot, and Olivier Doaré.
A ROS-based kinematic calibration tool for serial robots.
In *IEEE/RSJ International Conference on Intelligent Robots and Systems (IROS)*, 2023.

Stefan A. Sauter and Christoph Schwab.
Boundary Element Methods, volume 39 of *Springer Series in Computational Mathematics*.
Springer, Berlin, Heidelberg, 2011.

References III

Helmut Brakhage and Peter Werner.
Über das Dirichletsche Außenraumproblem für die Helmholtzsche Schwingungsgleichung.
Archiv der Mathematik, 1965.

F. Hecht.
New development in freefem++.
Journal of Numerical Mathematics, 2012.

J. C. Nedelec.
Curved finite element methods for the solution of singular integral equations on surfaces in R3.
Computer Methods in Applied Mechanics and Engineering, 1976.

References IV

Simon N. Chandler-Wilde, Ivan G. Graham, Stephen Langdon, and Euan A. Spence.
Numerical-asymptotic boundary integral methods in high-frequency acoustic scattering.
Acta Numerica, 21:89–305, 2012.

Robot acoustic footprint assessment

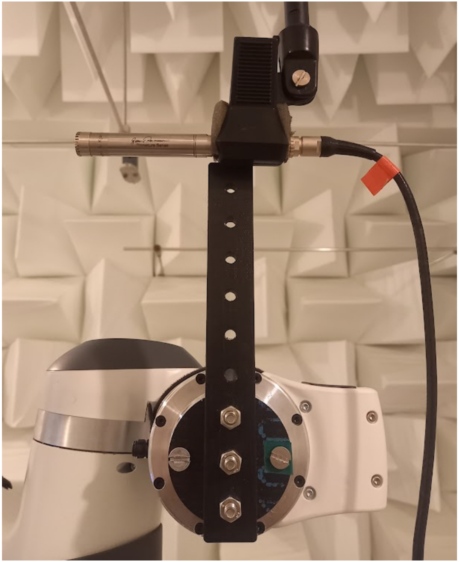

Robot acoustic footprint assessment

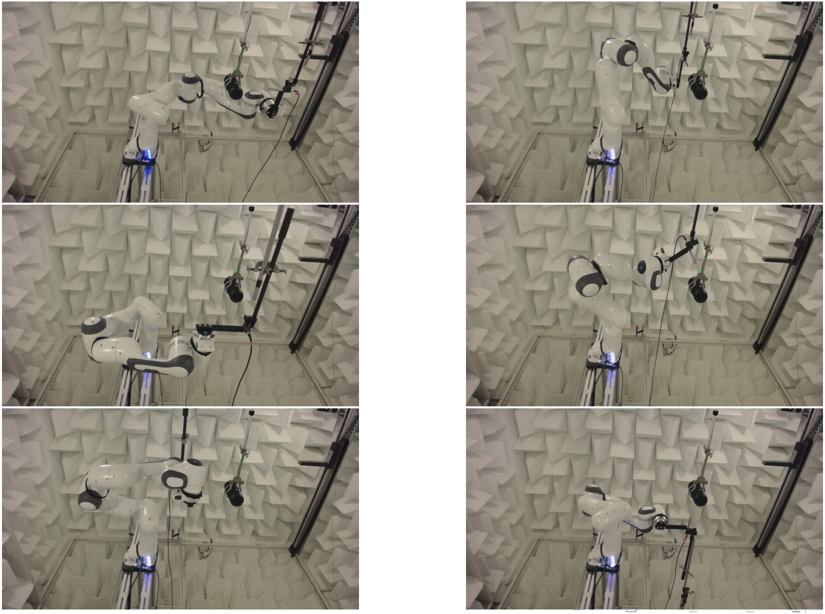

Example of robotized acoustic measurements

Click!